ANALYSIS OF SAR RESPONSE ANISOTROPIC BEHAVIOR USING SUB-APERTURE POLARIMETRIC DATA

L. Ferro-Famil[(1)], A. Reigber[(2)], E. Pottier[(1)], W. M. Boerner[(3)]

[(1)] *IETR Laboratory, UMR CNRS 6164, University of Rennes 1, Campus de Beaulieu, Bât. 11D, 35042 Rennes, France.*
E-mail: laurent.ferro-famil@univ-renne1.fr, eric.pottier@univ-rennes1.fr

[(2)] *Technische Universität berlin, Photogrammetrie & Kartographie, Strasse des 17. Juni 135, EB9, D-10623 Berlin, Germany*

[(3)] *UIC-EECS 900 W. Taylor St., SEL (607)W-4210, M/C 154, CHICAGO IL/USA-60607-7018*

ABSTRACT

Conventional SAR processing techniques generally assume that targets have a stationary behavior during the SAR integration. However, SAR sensors operating at lower frequencies, like L- and P-band, have a wide antenna characteristic in azimuth; i.e. during the formation of the synthetic aperture, multiple squint-angles are integrated to build the full-resolution SAR image. In this paper, a fully polarimetric sub-aperture analysis method is introduced. Using deconvolution, synthesized SAR images are decomposed into sub-aperture data sets, which correspond to the scene responses under different azimuthal look-angles. A statistical analysis of the polarimetric parameters permits to clearly discriminate media showing a non-stationary behavior during the SAR integration. Finally, a method is proposed, which eliminates the influence of azimuthal backscattering variations in conventional polarimetric SAR data analysis.

1. INTRODUCTION

The polarization properties of waves backscattered from a target are known to be highly related to its size, shape, geometrical structure and dielectric properties [1]. During the azimuthal integration, each scatterer is observed by the SAR sensor under a set of azimuthal look-angles, defined by the antenna's azimuthal aperture. Complex targets, characterized by anisotropic geometrical structures, may show a varying electromagnetic behavior, as they are illuminated from different positions. Some natural media, comporting periodic structures in the case of agricultural areas, or linear alignments of strong scatterers, are also susceptible to have varying polarimetric features during the SAR acquisition.
In this paper, a scene backscattering response is characterized using sub-aperture SAR data sets in the azimuth direction in order to analyze the responses of the whole observed scene under specific look-angles. A study of the evolution of its polarimetric properties during the SAR azimuthal integration allows to identify and to eliminate the influence of non-stationary scattering behavior to the polarimetric signatures.

2. SYNTHESIZED SAR IMAGE DECOMPOSITION PRINCIPLE

During SAR image formation, many low resolution echoes of a target, received under different squint angles, are integrated to form the full resolution SAR image. A single pixel in a SAR image, therefore, does not correspond to only one discrete line-of-sight, but to a certain range of angles limited by the azimuth antenna pattern. SAR imaging at lower frequencies, like L- and P-band, requires a wide angular distribution to achieve high image resolution. The azimuth look-angle, ϕ, is related to the wave number in azimuth k_x by :

$$k_x = \frac{2\omega}{c}\sin\phi \tag{1}$$

with ω denoting the carrier pulsation of the radar and c denoting the speed of light. Instead of processing a SAR image with the full resolution, it is also possible to process a set of images, each containing a different part of the SAR Doppler spectra., with a reduced resolution, but corresponding to different azimuth look-angles [2][3].
However, often raw data are not available and one has to deal with already processed SAR images. In this case, data have first to be transformed to the azimuth spectral domain by one-dimensional Fourier transforms (FFT). The Doppler spectrum is then split into several sub-apertures, each containing equally sized intervals of azimuth angles. Finally, all sub-apertures are transformed back to time-domain by inverse Fourier transforms (IFFT).
When having to deal with processed SAR data, special attention has to be paid to weighting functions, commonly used during SAR data processing or uncompensated azimuth antenna pattern. Therefore, it is necessary first to correct for potential spectral imbalances in the original, full-resolution SAR image. This can be easily achieved by calculating an average image spectrum in azimuth and then weighting each azimuth spectra with the inverse of the result. An appropriate weighting function can be individually applied before transforming them back to time-domain.

3. ANALYSIS OF AZIMUTHAL VARIATIONS OVER A NATURAL SCENE

An analysis of the sub-aperture images obtained from distinct parts of the azimuth spectrum permits to detect potential

angular variations in the backscattering behavior by comparison of independent sub-sets of the full-resolution image. Specific azimuthal look-angles, corresponding to non-stationarities, can then be located unambiguously in the Doppler spectrum. A trade-off has to be made concerning the choice of the number of sub-apertures. The resolution in time and frequency domains is adjustable by the number of sub-apertures. A large number enables a refined description of the data evolution during the azimuthal look-angle variation, while a smaller number of sub-apertures give a higher resolution in time-domain. The authors found that a number of eight sub-apertures offers a good compromise between the degree of spectral description and the spatial resolution.

3.1. Anisotropic polarimetric behavior

Polarimetric descriptors, widely used in natural media physical parameter retrieval procedures[4-6], permit to determine in a quantitative way the importance of eventual non-stationarities from an applicative point of view. Cloude and Pottier [1][7] introduced a polarimetric decomposition theorem of a distributed coherency matrix onto its eigenvector basis. From this decomposition are extracted two meaningful roll-invariant parameters: $\underline{\alpha}$, and H [1][7]. $\underline{\alpha}$ stands for the indicator of the mean scattering mechanism, while the entropy H is an indicator of the random behavior of the global scattering. The sub-aperture decomposition technique, introduced in the former paragraph, is applied to polarimetric SAR data acquired by the DLR E-SAR sensor, at L band, over the Alling test site, Germany. The considered scene is mainly composed of agricultural fields and forest. A urban area is located at the bottom left corner of the image while an isolated buildings may be observed in the top right of the scene.
The original image resolution is 2m in range and 1m in azimuth, corresponding to an azimuthal variation of the look-angle of approximately 7.5 degrees. In the following, the number of sub-apertures remains fixed to eight.
Fig. 1 shows an example of the sub-aperture decomposition over a particular area, corresponding to plowed fields. Images of the span and H and $\underline{\alpha}$ parameters are represented for different azimuthal look-angles and for the full resolution case. It can be observed in Fig. 1 that large variations in the scattering mechanism nature and degree of randomness occur as the azimuth look-angle changes. For particular azimuth look-angles, some fields show a sudden change of behavior. The span reaches a maximum value, while the polarimetric indicators H and $\underline{\alpha}$ are characterized by low values. Stripes in the span image indicate that coherent constructive and destructive interferences occur within the pixels and are characteristic of Bragg resonant scattering over periodic surfaces [8]. It was also observed that some point targets and linear structures, such as diffracting edges or road sides, have back-scattering properties susceptible to vary in

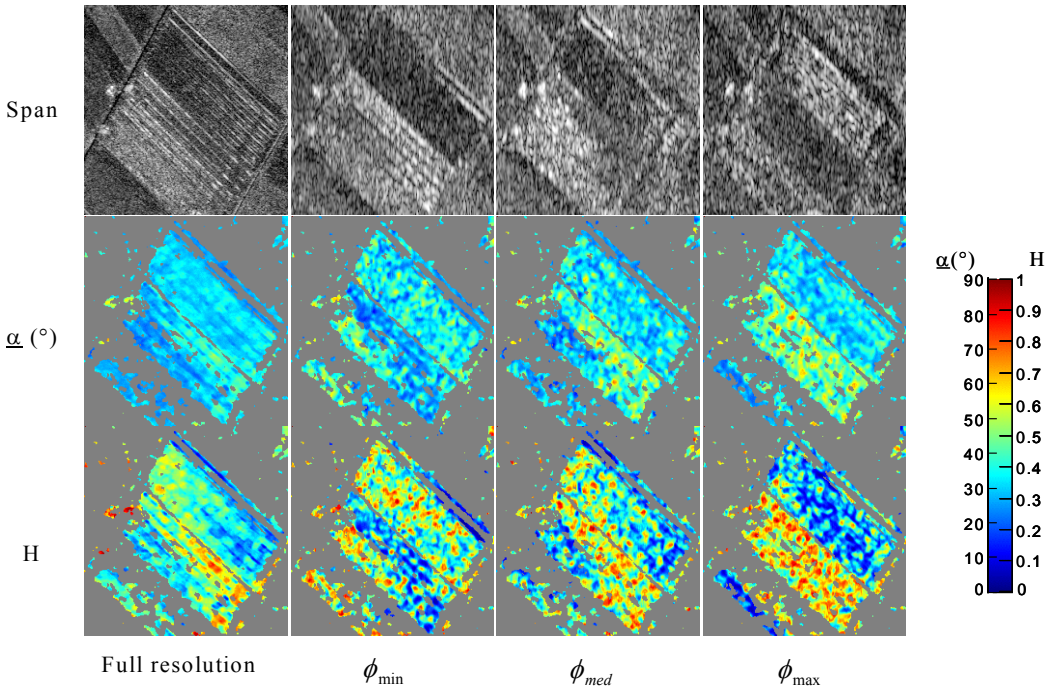

Fig 1: Polarimetric parameters over isolated fields at full resolution and after sub-aperture decomposition

a very significant way as the look-angle changes. In particular, fences consisting in a metallic net structure were found to present a scattering mechanism ranging from single bounce up to double bounce scattering depending on the SAR

azimuthal look-angle. In general, non-stationary targets have strongly anisotropic shapes, involving changes in the underlying scattering mechanism nature and randomness, as well as in the total backscattered power.
It is important to note, that forested areas have a constant behavior during the SAR integration. Back-scattering from forested areas is known to be, at L band, dominated by volume diffusion. The coherent integration of randomly scattered waves leads to a response characterized by a high intensity with a low degree of polarization but with isotropic features.

3.2. Bragg-resonance over natural surfaces

Bragg resonance phenomenon is due to the coherent summation of simultaneously constructive contributions of a set of scatterers and is likely to happen during the observation of periodic surfaces or irregular surfaces with a strong periodic component. The resonance condition can be written as a function of the incident wavelength, λ, as follows :

$$2k_y = n\frac{2\pi}{P} \quad \Rightarrow \sin\theta\cos\phi_o = n\frac{\lambda}{2P} \tag{2}$$

where k_y correspond to the component of the incident wave vector parallel to the ground and n is an unknown integer number. The local incidence angle is denoted θ, while ϕ_o represents the azimuthal angular difference between the observation position and the normal to the rows of the periodic surface.

According to (2), similar fields with different locations, i.e. corresponding to different incidence angles, or oriented along different directions, may resonate in different sub-apertures or not resonate at all, if the conditions mentioned earlier cannot be satisfied for any look-angle within the antenna azimuthal aperture. It follows from (2) that the occurrence of pixels affected by BRAGG-resonance increases with the SAR antenna azimuthal aperture. The joint dependence of the resonance condition on the incidence and azimuth angles can be observed on homogeneous fields having parts resonating in different sub-apertures. As the radar look-angle varies, the set of incidence angles satisfying (2) changes, leading to the apparition of sliding resonating stripes in the span image. This phenomenon can be observed on the sub-aperture images shown in Fig. 1. The width of the resonating stripes is fixed by the width of the sub-aperture Doppler spectrum, which defines the range of look-angle for the sub-aperture under consideration.

The values of polarimetric indicators of two resonating fields over the eight sub-apertures are plotted in Fig. 2. As the surface resonates, scattering mechanisms associated to low values for H and $\underline{\alpha}$ are weighted by a large intensity and strongly influence the nature of the full resolution scattering mechanism. The polarimetric indicators, within the sub-apertures unaffected by the BRAGG-resonance, are similar to the ones observed over stationary fields.

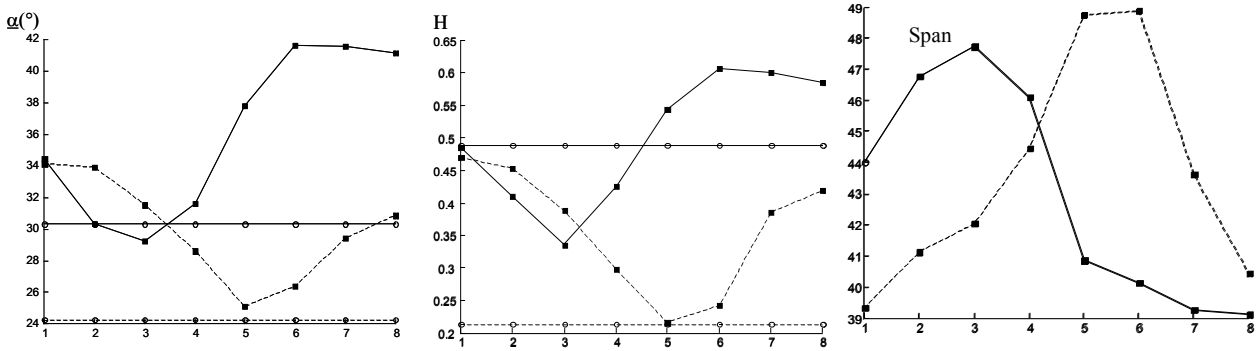

Fig 2 : Polarimetric parameters over two isolated fields, for each of the 8 sub-apertures. Solid lines correspond to Field 1, while dashed lines correspond to Field 2. Squares indicate parameters calculated for each sub-aperture and circles denote the corresponding full resolution value.

4. NON-STATIONARY TARGET DISCRIMINATION

A statistical analysis of the scene response over the different sub-apertures may is used to detect targets showing non-stationary behavior and locate their position in the azimuth spectrum by testing the statistics of a Maximum Likelihood (ML) ratio.

4.1. Maximum Likelihood detection

Each pixel of the SAR scene is associated to a set of sample coherency matrices, obtained from the different sub-apertures. It was shown that a sample n-look coherency matrix, $\mathbf{T}$, follows a complex Wishart probability function with n degrees of freedom, $W_C(n,\mathbf{\Sigma})$ [9][10]. A pixel has a stationary behavior if its R sub-aperture sample coherency matrices $\mathbf{T_i}$, with $i = 1,...,R$, follow the same distribution. In this case, the R coherency matrices fulfill the following hypothesis :

$$Hyp : \mathbf{\Sigma_1} = ... = \mathbf{\Sigma_R} \tag{3}$$

The validity of this hypothesis is tested by means of a maximum likelihood ratio Λ, built from the sub-aperture coherency matrices as follows :

$$\Lambda = \frac{\prod_{i=1}^{R} |\mathbf{T_i}|^{n_i}}{|\mathbf{T_t}|^{n_t}} \text{ with } n_t = \sum_{i=1}^{R} n_i \text{ and } \mathbf{T_t} = \frac{\sum_{i=1}^{R} n_i \mathbf{T_i}}{n_t} \tag{4}$$

The variable n_i represents the number of scattering vectors used to compute the sample coherency matrix $\mathbf{T_i}$. The hypothesis is accepted and the target is considered to be isotropic, with an arbitrarily chosen probability of false alarm P_{fa}, if :

$$\Lambda > c_\beta \quad \text{with } P_{fa}(c_\beta) = P(\Lambda \le c_\beta) = \beta \tag{5}$$

The testing requires the formulation of $P_{fa}(c_\beta)$, i.e. the calculation of the ML ratio statistics under the stationarity hypothesis mentioned in (3) [11][12]. This calculation cannot be done directly in an easy way. In [12] a way is proposed to derive an analytical expression of the statisticsby calculating the moment function of the ML ratio.
After many calculations, this probability may be expressed as:

$$P_{fa}(c_\beta) = 1 - \gamma_{inc}(f/2, -\rho\log(c_\beta)) - \omega_2[\gamma_{inc}(f/2+2, -\rho\log(c_\beta)) - \gamma_{inc}(f/2, -\rho\log(c_\beta))] \tag{6}$$

where $\gamma_{inc}(a,b)$ represents the incomplete gamma function of order a of b. One can note that the false alarm probability could also be written using the Chi-square function.

4.2. Location of non-stationarities in the azimuth spectrum

It was shown in the former paragraph that non-stationary targets could be discriminated using a ML ratio Λ, computed over the entire set of sub-aperture images. A similar approach can be applied to the location of the non-stationarities in the azimuth spectrum by comparing the contributions of each sub-aperture image in the global ratio.

A pixel showing a non-stationary behavior during the SAR azimuthal integration presents a set of coherency matrices that does not accomplish the hypothesis in (3), i.e. at least one the N_{sub} sample matrices does not belong to the global statistics. For each pixel, the sub-aperture sub_j, with $j \in [1...N_{sub}]$, corresponding to the most anisotropic behavior among the whole set, satisfies to the following relation :

$$sub_j = \arg\max \Omega_{N_{sub}-1}(sub_j) \tag{7}$$

where $\Omega_{N_{sub}-1}(sub_j)$ is a maximum likelihood ratio calculated over $N_{sub} - 1$ images, without incorporating the sub-aperture sub_j. For each pixel, it is then possible to iteratively discriminate, from an original set of R sub-apertures, the set corresponding to non-stationary behaviors. The procedure ends if the remaining sub-aperture describes a stationary behavior, or if a termination criterion is met. The user may wish to preserve a certain amount of the original resolution during the evaluation of the stationarity. In this case, the termination criterion consists in the comparison of the actual number of stationary sub-apertures with an arbitrarily fixed constant.

5. EXPERIMENTAL RESULTS

5.1. Detection of areas with anisotropic behavior

The previously proposed algorithm for detecting non-stationary behavior is applied to the polarimetric SAR data of the Alling test site. The resulting map of non-stationary pixels is presented in Fig. 3
As it can be seen, a substantial amount of pixels are found to have a non-stationary behavior during the SAR integra-

tion. The non-stationary pixel map indicates that many agricultural fields were affected by the Bragg resonance phenomenon. Complex targets and diffracting edges, whose scattering characteristics highly depends on the observation position, are discriminated in the urban areas as well as in the isolated building surroundings. Some linear targets are also found to have an anisotropic behavior, while forested areas have constant polarimetric features during the integration.The algorithm of localization of non-stationary behaviors algorithm is then applied to the detected problematic pixels. In Fig. 3 a map is presented, which indicates the location of the non-stationary sub-aperture of a pixel after one iteration of the localization algorithm. The color coding of Fig. 3 indicates the number of the sub-aperture, whose sample coherency matrix presents the lowest probability to belong to the global statistics.

It can be observed on many fields affected by BRAGG-resonance that some groups of pixels, belonging to a same field, have a maximum anisotropic behavior in different sub-apertures. This is a consequence of the sliding effect of the BRAGG on periodic structures described formerly. Repeated application of the localization algorithm reveal further problematic sub-apertures for a pixel. Resonances have a certain bandwidth, which might be wider than the bandwidth of a single sub-aperture. In this case more than one sub-aperture is necessary for an adequate description of the problem.

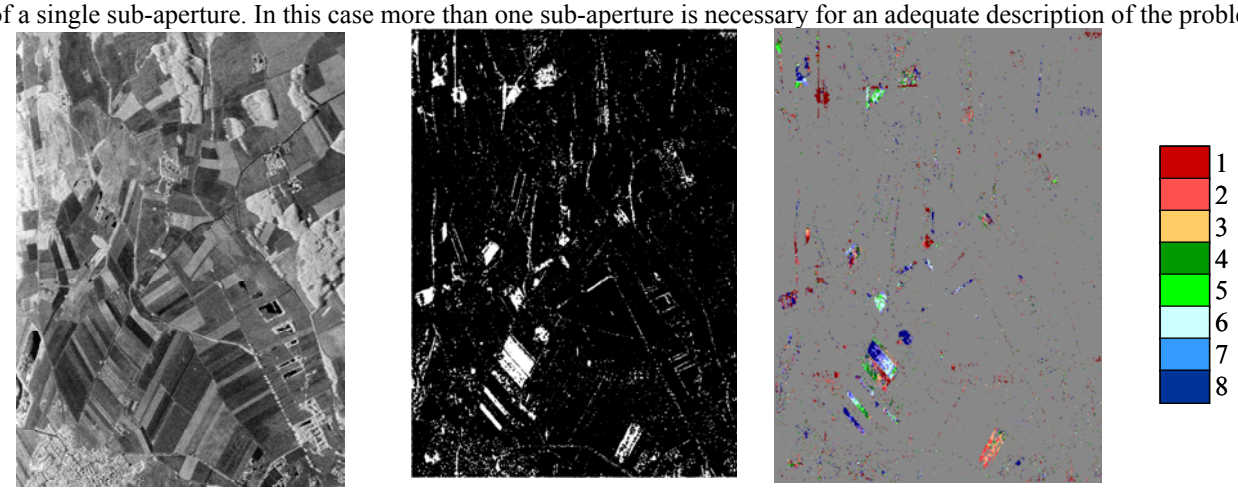

Fig 3 : Span image of the Alling site at L band (left), Non-stationary pixel map (center). Non-stationary pixels are represented in white, Location of the lowest probability sub-aperture among 8 original sub-apertures for each non-stationary pixel (right)

5.2. Sub-aperture Image Restoration

Once pixels with anisotropic behavior and the respective problematic sub-apertures are known, one can try to eliminate the anisotropic contributions, in order to improve the retrieval of physical properties from polarimetric data partially affected by furtive contributions. An efficiicient restoration approach consists in equalizing the amplitude of all sub-apertures to the average amplitude of the unaffected sub-apertures. In fact, this leaves the potentially erroneous phase values of affected sub-apertures untouched, but due to their smaller amplitude weighting in the SAR integration, their effect on the result is much less significant Coorrupted polarimetric scattering coefficients are corrected by estimating the properties of a global scattering mechanism over the stationary sub-apertures. A stationary coherency matrix is constructed using the contributions from all the stationary sub-apertures. A unitary scattering vector may then be estimated from the average scattering parameters, $(\underline{\alpha},\underline{\beta},\underline{\delta},\underline{\gamma})$. The corresponding scattering matrix is weighted by the equalized amplitude and the absolute phase. In Fig. 6, polarimetric parameters of the full-resolution SAR image after restoration are shown. It is clearly visible that the variations due to non-stationary scattering are not present anymore. The image quality is comparable with the original one, shown in Fig. 2. Differences between polarimetric descriptors, entropy and $\underline{\alpha}$, evaluated in the original and restored images can be observed. Maximal variations of 70° and 0.8 are observed, over anisotropic point scatterers, for $\left|\Delta\underline{\alpha}\right|$ and $\left|\Delta H\right|$ respectively. Over non-stationary fields affected by Bragg-scattering, the average variations in $\left|\Delta\underline{\alpha}\right|$ and $\left|\Delta H\right|$ are respectively 7° and 0.2. Such values are significant with respect to the ranges of the polarimetric indicators, which in case of backscattering over rough surfaces equal 40° for $\underline{\alpha}$ and to 0.9 for the entropy.

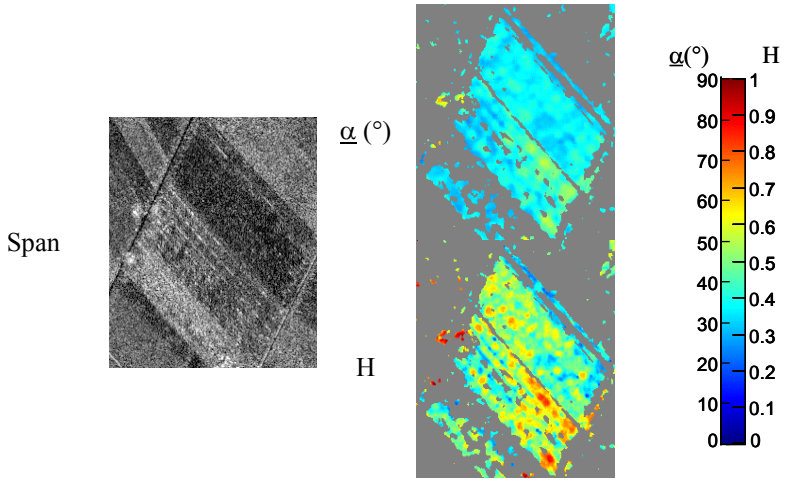

Fig 4: Polarimetric parameters over isolated fields at full resolution after restoration

6. CONCLUSION

Sub-aperture analysis of fully polarimetric SAR data is an interesting and important way to characterize the scattering behavior of many targets. As shown in this paper, the effect is very common and cannot be neglected in a polarimetric analysis without introducing severe errors. Particularly, the characterization of agricultural scenes with polarimetric descriptors can be heavily influenced by Bragg scattering on periodic surface. Physical parameters like for example soil moisture and roughness can be extracted erroneously on such surfaces.

In this paper a method is proposed to detect problematic sub-apertures, i.e. azimuthal look-angles corresponding to non-stationary behavior using multi-image ML test statistics, based on the Wishart probability distribution. Results of this method can be used to minimize the influence of azimuthal backscattering variations in conventional polarimetric SAR data analysis. Polarimetric parameters extracted from restored data sets show, for non-stationary agricultural fields, average variations of 7° for $\underline{\alpha}$ and 0.2 for the entropy. Such variations have to be compared to the ranges of the polarimetric indicators, equal to 40° for $\underline{\alpha}$ and to 0.9 for the entropy.

REFERENCES

[1] S. R. Cloude and E. Pottier: “An Entropy Based Classification Scheme for Land Applications of Polarimetric SAR ", *IEEE Transactions on Geoscience and Remote Sensing*, Vol. 35, No. 1, pp 68-78, January 1997.

[2] T.L. Ainsworth, R.W. Jansen, J.S. Lee and R. Fiedler: ”Sub-aperture analysis of high resolution polarimetric SAR data”, *Proceedings of IGARSS ’99*, Vol. 1, pp. 41-43, 1999

[3] A. Moreira: “Real-time Synthetic Aperure Radar (SAR) Processing with a new Subaperture Approach”, *IEEE Transactions on Geoscience and Remote Sensing*, Vol. 30, No. 4, pp. 714-722, July 1991

[4] I. Hajnsek, "Inversion of Surface Parameters using Polarimetric SAR", Ph.D. Thesis, University Jena, Institute of Geography, Department of Geoinformatik, Jena, Germany, September 2001.

[5] L. Ferro-Famil,"Multi-temporal and Multi-frequency Remote Sensing of Natural Media using Polarimetric SAR data", Ph.D. Thesis, University of Nantes, France, December 2000.

[6] S. Allain, L.Ferro-Famil, E. Pottier, I. Hajnsek," Extraction of Surface Parameters from Multi-frequency and Polarimetric SAR Data", International Geoscience and Remote Sensing Symposium 2002, Toronto, Canada, June 2002.

[7] S. R. Cloude, E. Pottier " A Review of Target Decomposition Theorems in Radar Polarimetry ", *IEEE Transactions on Geoscience and Remote Sensing*, Vol. 34, No. 2, pp 498-518, September 1995.

[8] H.A. Yueh, R.T. Shin, and J.A. Kong, "Scattering from randomly perturbed periodic and quasi-periodic surfaces", *Progress in Electromagnetic Research*, Elsevier, Vol. 1, pp. 297-358, 1988

[9] N. R. Goodman, “Statistical analysis based on a certain multi-variate complex Gaussian distribution (an introduction),” *Annals of Mathematical Statistics,* Vol. 34, pp. 152–177, 1963.

[10] J.S. Lee, M.R. Grunes, R. Kwok, " Classification of multi-look polarimetric SAR imagery based on the complex Wishart distribution ", *International Journal of Remote Sensing*, Vol. 15, No. 11, pp 2299-2311, 1994.

[11] K. Conradsen, A. A. Nielsen, J. Schou, H. Skriver, "Change Detection in Polarimetric SAR Data and the Complex Wishart Distribution", International Geoscience and Remote Sensing Symposium 2002, Toronto, Canada, June 2002.

[12] R. J. Muirhead "*Aspects of Multivariate Statistical Theory*", John Wiley and Sons, New-York, May 1982.